J Ther Eng, Vol. 12, No. 2, pp. 519−531, March, 2026

Journal of Thermal Engineering
Web page info: https://jten.yildiz.edu.tr
DOI: 10.14744/thermal.0001099

Research Article

Experimental investigation of a low-cost evacuated tube in a parabolic trough collector with and without porous insert

Pooja RAVAL[1,*], Bharat RAMANI[2], Karan MOTWANI[3], Nikhilkumar CHOTAI[3]

[1]*Gujarat Technological University, Gujarat, 380001, India*
[2]*Principal, LTIET, Gujarat, 360001, India*
[3]*Department of Mechanical Engineering, Marwadi University, Gujarat, 380001, India*

ARTICLE INFO

Article history
Received: 13 February 2025
Revised: 16 April 2025
Accepted: 12 May 2025

Keywords:
Circular Ring Wire Mesh Insert; Evacuated Tube; Nusselt Number; Parabolic Trough Collector; Thermal Efficiency

ABSTRACT

This research paper addresses the challenges of high upfront cost, maintaining vacuum, limited configurations and manufacturers, and fluid thermal retention in the evacuated receiver tube used in parabolic trough collector. These challenges affect the collectors cost and efficiency, which lowers its acceptance for the industrial market. Two attempts have been made to overcome this issue: developing an in-house evacuated tube of the specific configuration with locally available materials to reduce the cost. Furthermore, a novel porous insert is designed and examined inside the tube to improve fluid thermal retention, which will enhance the overall efficiency of the collector. An in-house developed evacuated tube with a notched circular ring porous insert is examined experimentally. The experimental tests were conducted using a manually tracked mechanism with a 2.36 m^2 aperture area and a 0.50 m focal length, utilizing water as the heat transfer fluid. Performance was evaluated with and without inserts at varying mass discharge rates (0.04, 0.06, and 0.08 kg/s), considering parameters such as Nusselt number, outlet fluid temperature, heat gain and thermal efficiency. The results demonstrate that the receiver tube with inserts significantly outperforms the plain tube (without insert). At higher mass flow rates, the insert-enhanced thermal efficiency is 31.2% and 20.46% in the Nusselt number. Also, a higher outlet fluid temperature is obtained in a tube with an insert, indicating improved thermal retention. This study establishes that incorporating novel inserts and developing in-house evacuated tube can be a viable solution for optimizing the cost and performance of the collector.

Cite this article as: Raval P, Ramani B, Motwani K, Chotai N. Experimental investigation of a low-cost evacuated tube in a parabolic trough collector with and without porous insert. J Ther Eng 2026;12(2):519−531.

INTRODUCTION

In parabolic trough collector (PTC), the receiver tube is considered to be the crucial component of the system. In general, the sun rays from the sun are concentrated on the receiver tube with the help of the reflector, which is placed at the focal distance from it [1]. The working heat

***Corresponding author.**
*E-mail address: pmghodasara@gmail.com

This paper was recommended for publication in revised form by Editor-in-Chief Ahmet Selim Dalkılıç

transfer fluid (HTF) is passed from the heating element or tube, which collects the thermal energy from the peripheral surface of the tube [2]. The thermal energy collected by the working fluid can be helpful for industrial and commercial applications. The importance of the receiver tube in PTC becomes significant due to its cost and efficiency. The cost of the receiver tube can be nearly 30 to 40% as compared to the overall cost of the system [3]. This cost consists of metal and glass tubes, coating, vacuum insulation, sealing, manufacturing and assembly. Out of this, vacuum insulation, sealing and coating are major components that make the receiver tube more expensive. On the other hand, including these three components on the receiver tube is a very vital part from the efficiency point of view.

Selective coating on the receiver tube, which has high absorptivity and low emittance, is selected [4]. Absorptivity helps to absorb more concentrated radiation from the sun, which ultimately maximizes the heat gain of the receiver tube and causes a rise in the temperature of the receiver surface and HTF. The low emittance property of the coating helps to decrease the heat losses due to an increase in the temperature of the tube [5]. This coating includes complex chemical depositions, which require advanced technologies, which makes this coating expensive [6-7].

Furthermore, vacuum insulation and sealing between metal and glass tubes reduce the conduction and convection losses from the receiver tube at higher temperatures. Sustaining a vacuum for a long time and managing the thermal stress of the receiver tube with heating and cooling requires precise manufacturing, which adds complexity and high cost [8].

Evacuated receiver tube with double side opens are very expensive compared to the evacuated tube used in the non-concentrating collector. The reason for this is the lower demand in the market, less production, and very limited manufacturers available globally. Evacuated tube used in non-concentrating collectors is designed for low-temperature applications up to 150°C. In contrast, the evacuated tube used in PTC is designed for high-temperature applications up to 400°C [9]. It has been noticed that due to the limited manufacture of such evacuated tube in the world, the additional cost of importing the receiver tube of specific configurations from different parts of the country will make it more expensive. Further, there is also the possibility of breaking glass tube due to fragile material and the loss of vacuum of the evacuated tube during adverse working industrial conditions. Figure 1 indicates the evacuated tube used in PTC.

Therefore, the authors have attempted to develop an in-house double-end open evacuated receiver tube for small PTC in the present experimental work. The evacuated tube is described in detail in the next section.

The above discussion states the importance of an evacuated tube for improving the efficiency of the PTC by restricting heat losses from the external part of the tube. The next focus of the authors was to emphasize the

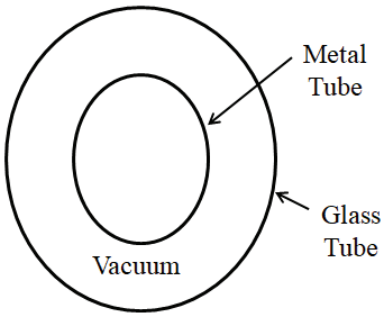

Figure 1. Indicates evacuated tube used in PTC.

performance by internal means of the receiver tube. The authors have recognized two types of methods from various literature reviews, such as the use of nanofluid [10] and inserts [11]. The use of nanofluid can enhance the working fluid conductivity, which can boost the thermal gain and overall efficiency of the solar collector. Hussein et al. [12] evaluated the thermal performance of the flat plate collector with nanofluid as CuO/H_2O over three months in Iraq. Results indicate that 1% CuO/H_2O nanofluid improves the collector efficiency by 32%, and 11.3% performance surpasses was observed while using pure H_2O. Ajbar et al. [13] carried out a simulation analysis on PTC with eight hybrid nanofluids. The thermal efficiency of PTC in all hybrid nanofluids was found to be better compared to the base fluid as Syltherm 800. Challenges such as nanofluid stability, chances of corrosion and erosion of inside tube material, and thermal instability at high temperatures may affect the performance of the PTC for a long time [14].

Next, a literature review was focused and conducted on inserting an insert in the receiver tube to improve the internal heat transfer coefficient of the fluid, which can lead to internal heat gain of the fluid and the overall performance of the PTC. Generally, two types of inserts are categorized: active and passive [15]. From the literature, authors have come across that active types of inserts are not more favorable due to their complexity and high cost [16]. Meanwhile, passive types of insert enhance thermal energy transfer and improve the system performance without requiring any external energy.

Various researchers have proven that inserts inside the receiver significantly improve the heat transfer enhancement in solar thermal systems compared to the plain tube. Twisted tapes [17], [18], wire coils [19], fins [20], [21], wire mesh [22], [23], perforated plates [24], and porous inserts [25] are found to be passive inserts, which various authors have researched. Most of the inserts have been researched in the field of heat exchangers and solar thermal systems. Several experimental and numerical studies have been conducted on PTC using inserts such as twisted tapes and fins; however, most investigations have been limited to numerical analysis. Farhad et al. [26] carried out a numerical study involving

dual twisted tape inserts within a Reynolds number range of 10000 to 20000. The Nusselt number was found to be 19.58% higher compared to a plain tube, demonstrating enhanced heat transfer performance [26]. Piyush et al. [27] performed an experimental study on a solar-based air heater utilizing dual-arc artificial roughness, which revealed a significant enhancement in heat transfer performance. The Nusselt number was found to increase by a factor of 2.27 compared to a conventional solar air heater. However, this improvement was accompanied by a substantial rise in pressure drop, which was 3.10 times higher than the plain solar air heater. Karunaraja et al. [28] carried out an experimental investigation on solar drying using a solar tunnel dryer under the meteorological conditions of Negamam. The solar tunnel dryer using thermal storage materials exhibited 2–3% higher thermal efficiency than no storage material. Sand as a thermal storage material was found to be the most effective in this study. Prem et al. [29] conducted a review study, presenting various techniques for enhancing the efficiency of solar stills. Among these, passive augmentation techniques were highlighted as an effective approach for converting polluted water into potable water.

Furthermore, these inserts perform differently, whether they are solid or porous. Twisted tapes, conical displacers, and fins are considered to be part of the solid inserts. Such types of inserts have high durability and low-pressure drop, but they can cause high fouling resistance and are heavier in weight. Meanwhile, porous inserts have their own advantages, such as being light in weight and generating turbulence with moderate pressure drop with chances of low to moderate fouling resistance.

Pooja et al. [23] experimentally studied the behaviour of the wire mesh inside the receiver tube and compared its results with that of the plain tube. Two types of inserts were studied under the laboratory setup: wire mesh twisted tape (WMTT) and circular ring wire mesh (CRWM). Parameters such as friction factor, Nusselt number, and performance evaluation criteria (PEC) were determined to compare the various inserts. Figure 2 (a) and (b) illustrate WMTT and CRWM inserts. Experimental results show that wire mesh performs better as compared to plain tube. Meanwhile, the efficacy of CRWM inserts has been found to be more promising than that of WMTT. Although CRWM demonstrates a higher Nusselt number, it also results in a greater pressure drop. In contrast, WMTT shows a slightly improved Nusselt number, while maintaining a relatively lower pressure drop. The PEC for both inserts was evaluated to assess overall performance, revealing that CRWM exhibits a superior PEC compared to WMTT. Therefore, in the current research paper, the authors have attempted to investigate the other configuration of CRWM for optimizing the thermal performance of the PTC.

This research paper consists of two broader aims: first, develop a notch-based CRWM inserts for improving the thermal retention of the fluid and second, fabricate low-cost in-house evacuated receiver tube for optimizing the cost of the PTC. An experimental investigation of in-house developed tube with and without insert is carried out to evaluate the performance of the PTC. The following subsections of this paper discuss the development of an in-house evacuated tube, CRWM insert, design and experimental part of PTC, data analysis and validation, and results and discussions.

DEVELOPMENT OF IN-HOUSE EVACUATED TUBE FOR PTC

Evacuated tube consists of four major parts, i.e. metal tube, glass tube, coating and vacuuming between metal and glass tube. Metal tube must be selected based on higher thermal conductivity, corrosion resistance, temperature

(a) WMTT

(b) CRWM

Figure 2. (a) and (b) Illustrates WMTT and CRWM inserts.

Figure 3. Illustration of in-house developed evacuated receiver tube.

range and mechanical strength. The most common materials used in solar thermal collectors are copper and stainless steel [30]. It has been observed that stainless steel as a material is more suitable for higher temperature applications above 250°C due to its strong mechanical properties. At the same time, copper is the best option for low to medium-temperature applications [31]. Secondly, a glass tube made of borosilicate is generally used to cover the metal tube, which has high transmittance and is capable enough to withstand high temperatures. The vacuum is created in this concentric metal and glass tube, which maintains thermal insulation to prevent energy losses at high temperatures. It also protects the metal tube and its coating from the surrounding environment.

Next, coating with thickness in a range of 0.2 to 2 microns is used on the external peripheral surface of the receiver tube, which helps to enhance absorption of the sun radiation and simultaneously reduces thermal energy emission losses with an increase in temperature. Black chrome and matte black paint coating can be used on the external peripherals surface of the tube, which is locally available, less expensive, and easy to apply [5]. Coatings, such as ceramic-metal composites, carbon or graphene-based, titanium nitride oxide, etc., are also examined in PTC [32]. Lastly, an enclosure of metal and glass tubes with coating is vacuumed and sealed for thermal insulation. Different types of sealing, such as glass to metal, metal bellows, elastomer, epoxy resin, brazed sealing, and compression sealing options, are available to make a perfect vacuum sealing. Selection of sealing is based on temperature range, thermal stability and vacuum retention [33]. From the literature review, it was noted that sealing such as epoxy resin, compression sealing, and elastomer can withstand up to a temperature range of 150 - 200°C. While glass-to-metal, brazed sealing and metal bellows are more suitable for higher temperature ranges up to 500°C.

In the present study, a metal tube made of copper material was selected, with inner and outer diameters of 22 mm and 25 mm and an effective tube length of 1000 mm. Illustration of an in-house developed evacuated receiver tube is shown in Figure 3. A locally available matt black coating was applied on the external surface of the copper tube. Borosilicate glass tube having inner and outer diameter of 47 mm and 50 mm were selected to form an enclosure on the metal tube. Finally, the rubber seal was cut and fitted according to the space between the copper and glass tube. A heat-resistant adhesive was applied to enhance the bonding between the contact surface of the seal and copper. The Glass tube was slid and rotated over the copper tube to maintain a proper gap, disturbing the adhesive uniformly and preventing air pockets from forming. A vacuum pump was used to evacuate air and obtain the desired pressure level between the copper and glass tube to integrate the vacuum seal. The vacuum pressure of -25 cm of Hg, equivalent to -0.3333 bars, was kept between enclosures. Pressure monitoring was done for two continuous days to ensure the vacuum and seal between glass and metal were tightened, ensuring leak detection. Figure 4 highlights the vacuum process conducted in the laboratory.

Circular Ring Wire Mesh Insert

Wire mesh is a porous type of insert used in the present study to examine its impact on the heat transfer performance of the PTC. Wire mesh of stainless steel with 18 pores per inch (PPI) (70% porosity) was selected due to being readily available in the local market. It was cut into a circular ring with the help of tin spins and fitted into the circular rod of 3 mm diameter and 1000 mm length. Twenty numbers of CRWM were located on the circular rod with a

Figure 4. Highlights the vacuum process conducted in the laboratory.

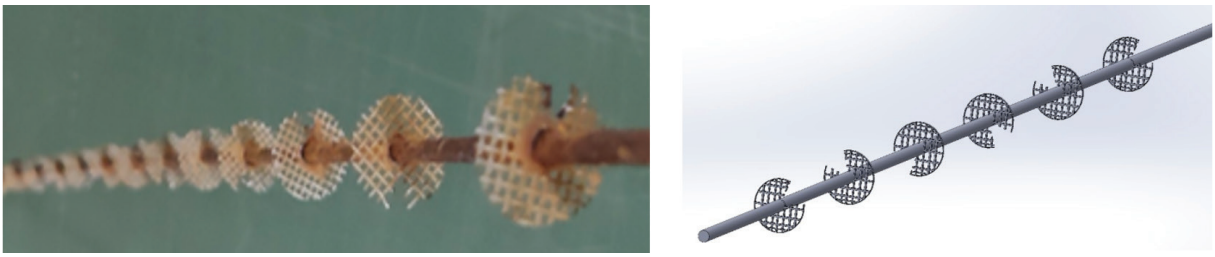

Figure 5. (a) and (b) Represents real and CAD model of circular ring wire mesh-18 PPI.

pitch distance of 50 mm. Furthermore, a V-notch cut was made in the circular ring, generating more turbulence and a larger surface area to increase heat transfer and help minimize the pressure drop. Real and CAD models of circular ring wire mesh-18 PPI are shown in Figure 5 (a) and (b).

Design of Parabolic Trough Collector

The concept design of the parabola is demonstrated in Figure 6. The PTC contains of a parabolic reflector with an eccentricity equal to one, designed to concentrate all sun radiation on the focal point. The receiver tube is located on the focal point, which absorbs the concentrated radiation. Generally, glass or aluminum sheets with high reflectivity are selected for a parabolic reflector. Parameters such as focal length, aperture size, rim angle, receiver tube diameter, and concentration ratio can be analyzed while designing PTC. The following equations (1 to 4) were used to design PTC [34]. The specifications for the design PTC are shown in Table 1.

Aperture area of the collector can be calculated using equation (1),

$$Aperture\ Area = Length\ of\ collector(W) * Width\ of\ parabola(l) \quad (1)$$

Surface area of receiver tube can be determined using equation (2),

$$Receiver\ area = \Pi * d_{go} * L \quad (2)$$

Where, d_{go} = diameter of the glass tube and L = glass tube length

Concentration ratio can be calculated using equation (3) [33],

$$CR = \frac{Aperture\ area}{Receiver\ area} = \frac{(W - d_{go})\ * l}{\Pi * d_{go} * L} \quad (3)$$

Focal point of the parabola can be calculated as mentioned in below equation (4),

$$F = \frac{W}{4 * tan\Phi/2} \quad (4)$$

Where, Φ = rim angle

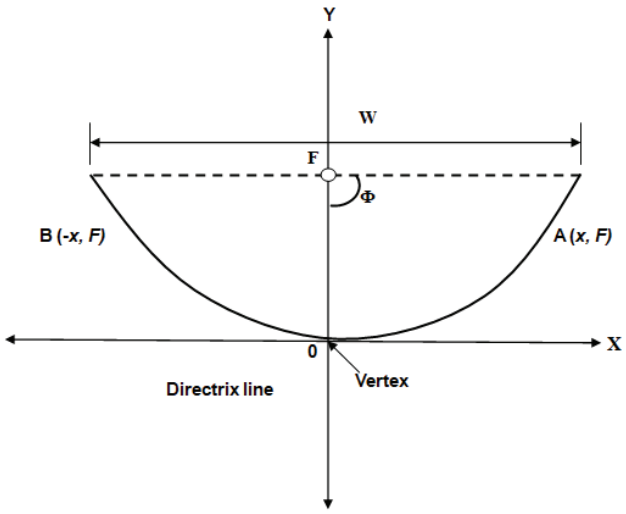

Figure 6. Demonstrates concept design of the parabola.

Table 1. Specification of PTC

Parameter	Value
Aperture width	1.865 m
Aperture area	2.36 m^2
Parabola length	1.3 m
Focal length	0.50 m
Rim angle	90°
Concentration ratio	15.03

Experimental Setup and Procedure

The experimental setup was fabricated and installed at Marwadi University, Rajkot, which is at 22°18'N latitude and 70°47'E longitude. The setup consists of a parabolic-shaped mirror reflector, evacuated receiver tube, inlet and outlet fluid thermocouple, pyranometer, anemometer, temperature gun, data logger, and miscellaneous accessories for fitting.

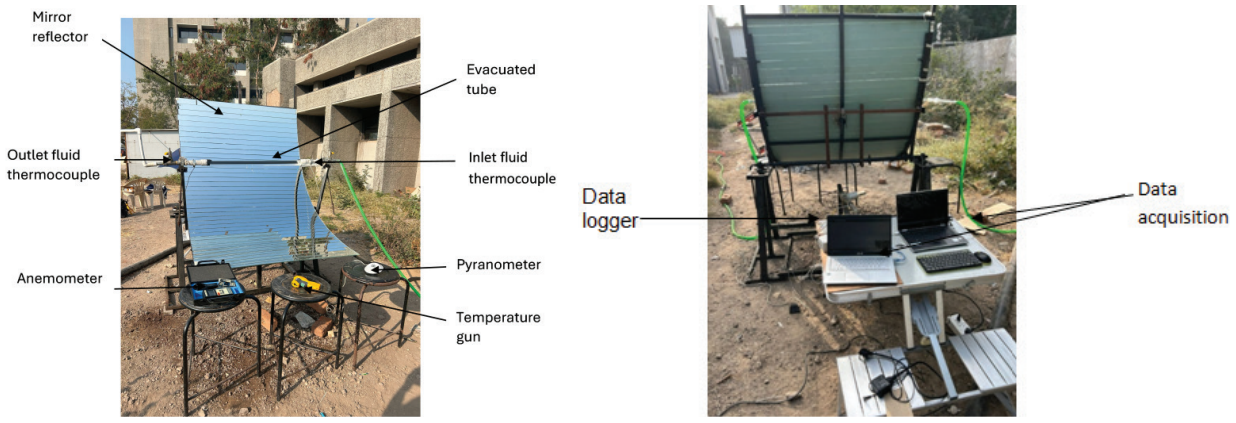

Figure 7. Experimental setup of PTC.

The PTC was installed on the ground and oriented southward with manual tracking (east to west) to ensure uninterrupted solar radiation. The copper receiver tube, with a diameter of 25 mm, was coated with matte black and mounted coaxially within a glass envelope that was evacuated to minimize heat loss, as depicted in Figure 3. Ro water was used as the HTF and properties are calculated at the bulk mean temperature. K-type thermocouples were connected at both ends of the tube to measure the fluid inlet and outlet temperature. The ends of the receiver tube were insulated with fiber wool to avoid thermal losses. A pyranometer (Class C) was employed to monitor solar radiation throughout the experiment. To measure the wind velocity and ambient temperature of the surrounding atmosphere, an anemometer was used. The average surface of the receiver tube was measured with the help of an infrared thermometer, which is also known as a temperature gun. Lastly, a data logger was used to record the fluid temperature reading and solar radiation for an interval of every 1 minute. The experimental setup of PTC is shown in Figure 7.

Experiments were performed on the PTC in January 2025 from 9.30 am to 4.30 pm. Two types of cases are examined in PTC: plain tube (without insert) and tube having notched CRWM insert. Data were collected under consistent ambient conditions and solar flux to facilitate a fair performance assessment of both cases. The study was conducted under three different discharge rates to judge the performance of the evacuated receiver tube with and without the insert. The discharge rate was measured using a calibrated beaker, and a flow control valve was used to adjust the flow rate. The experiment begins by allowing an inlet of water from one side with a known mass discharge rate to pass through the other end of the evacuated receiver

Table 2. Parameters and equations for data reduction

Parameters	Equation	Unit	Equation number
Useful heat gain (Q_u)	$Q_u = \dot{m} * c_p * (T_{fo} - T_{fi})$	W	(5) [35]
Heat transfer coefficient (h)	$h = \frac{Q_u}{A_r(T_{sur} - T_m)}$	W/m²K	(6)
Bulk fluid temperature (T_m)	$T_m = (T_{fo} + T_{fi})/2$	K	(7)
Nusselt number (Nu)	$Nu = \frac{hd_i}{k}$	-	(8) [35]
Dittus-Boelter correlation for turbulent flow	$Nu = 0.023(Re)^{0.8}(Pr)^{0.4}$	-	(9)
Reynolds number	$Re = \frac{\rho * v * d_i}{\mu}$	-	(10)
Prandtl number	$Pr = \frac{\mu * Cp}{k}$	-	(11)
Thermal efficiency	$\eta = \frac{Q_u}{I * A_p}$	-	(12)

tube. Manual tracking of PTC in the east-to-west direction was continuously carried out to concentrate radiation on the receiver tube. The performance parameters, such as the Nusselt number, outlet fluid temperature, heat gain and thermal efficiency, were assessed to identify the significance of the insert in PTC.

Data Analysis and Validation

For the calculation and analysis of the data, reading from all instruments was considered on hourly basis. The equations and parameters applied during data processing are presented in Table 2.

Figure 8 represents a comparison of the experimental and theoretical calculated Nusselt number. The Dittus-Boelter correlation for the Nusselt number mentioned in equation (9) was used to validate the turbulent flow behavior within the tube. These equations are relevant for fully developed turbulent flow conditions. The data used for the experimental Nusselt number was obtained across two mass discharge rates (0.06 and 0.08 kg/s) under nearly identical solar heat flux conditions (760 W/m^2). The mass discharge rate of 0.04 kg/s is not considered here in the validation due to the Reynolds number coming to less than 4000, which does not apply to the Dittus-Boelter equation. The data presented in Fig. 8 exhibits a strong correlation with the theoretical models, with deviations of ±2.6%. Furthermore, the results also indicate with an increase in Reynolds number, the Nusselt number shows a corresponding amplifies, suggesting an enhancement in convective heat transfer. These observations validate the accuracy and reliability of the experimental setup, confirming its suitability for the study.

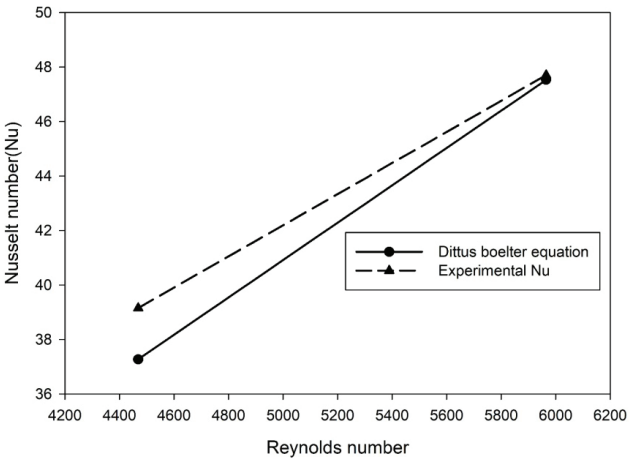

Figure 8. Comparison of experimental and theoretical Nusselt number.

Measurement of Uncertainty

This section outlines the inherent uncertainties associated with the experiment. Various instruments, including the thermocouples, solar pyranometer, flow meter, and data logger are employed to gather data during the test. The statistical uncertainty X (z) of the variables used in the data analysis can be calculated from the equation (13), where Y (z) represents the accuracy of the components. Additionally, the uncertainty for F (b) can be determined using equation (14) [36]. Table 3 provides the accuracy and uncertainty of devices. The cumulative uncertainty of the experiment is 1.34%.

$$X(z) = \frac{Y(z)}{\sqrt{3}} \tag{13}$$

$$F(b) = \sqrt{(A)^2 + (B)^2 + (C)^2 + (D)^2} \tag{14}$$

Where *A, B, C* and *D* are uncertainty in solar pyranometer, thermocouple, flow rate and data logger acquisition respectively.

RESULTS AND DISCUSSION

Solar Flux with Time

The data presented in Figure 9 demonstrates the variation in solar flux over several days, measured between 9:30 am and 4:30 pm under no cloud conditions at Marwadi University, Rajkot (22°18'N latitude and 70°47'E longitude) in January 2025. The data selected for processing corresponds to the six different days with the least cloud cover. It is important to note that, on all selected days, the overall solar energy received by the collector was nearly identical. The maximum solar flux was available between 12.30 to 1.30 pm and began to fall till 4.30 pm. The average solar fluxes received during the peak solar noon (12.30 to 1.30 pm) were 863 W/m^2.

Table 3. Accuracy and uncertainty of measuring devices

Instrument	Unit	Accuracy	Uncertainty (%)
Solar pyranometer	W/m^2	± 2	1.154
K type thermocouple	°C	± 0.25°C	0.144
Flow rate	LPM	± 0.06	0.034
Data logger acquisition	°C	<0.02	0.0115

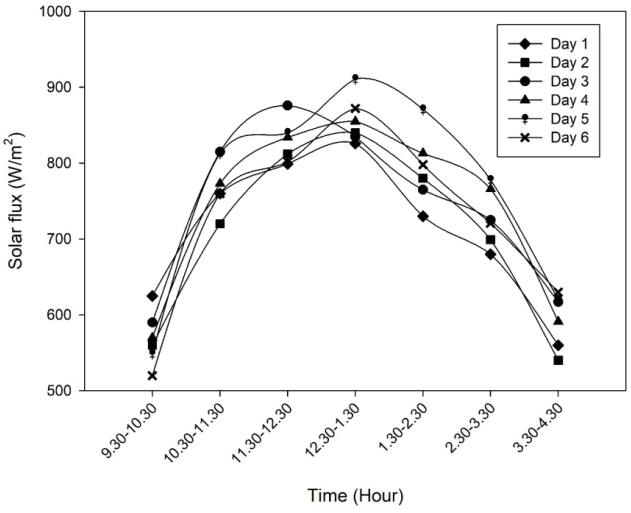

Figure 9. Solar flux variation with time at different days.

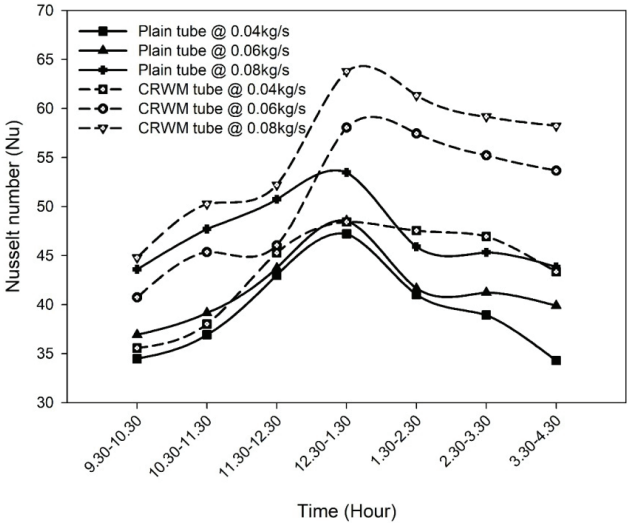

Figure 10. Comparison of Nusselt number with time at different mass discharge rates between plain and CRWM inserted tubes.

Impact of Mass Discharge Rates on Nusselt Number in the Case of Plain and CRWM Inserted Tubes

Figure 10 shows the comparison of the Nusselt number between a plain and CRWM inserted tube at three different mass discharge rates. It can be analyzed from the figure that as the mass discharge rate rises, the Nusselt number increases for both the plain and CRWM tubes. This trend is due to the rise in Reynolds number with the increasing mass discharge rate, which in turn enhances the Nusselt number. The highest Nusselt number is observed between 12:30 to 1:30 pm when the solar flux is at its peak. It can also be noted that tube with insert have a higher Nusselt number compared to plain tube in all mass discharge rates.

Table 4 presents the percentage gain in the average Nusselt number between plain and CRWM inserted tubes across all mass discharge rates. The percentage gain in the average Nusselt number is 20.46%, 17.64%, and 10.6%, with respective mass discharge rates of 0.08, 0.06, and 0.04 kg/s. These values clearly signify two key trends: first, a higher mass discharge rate will approach a higher Nusselt number, and second, the use of inserts in the tube has a higher Nusselt number as compared to the plain tube.

Impact of Mass Discharge Rates on Outlet Fluid Temperature in the Case of Plain and CRWM Inserted Tubes

Figure 11 presents the variation of outlet fluid temperature for various mass discharge rates considered in the present study for both the plain and porous insert. It can be observed that fluid outlet temperature increases with the rise in time. Solar radiation attains the highest value around 2 pm and then slowly decreases. It is further noted that the outlet fluid temperature varies from 23°C to 32°C for the tube with insert, and the same is from 21°C to 29°C for a tube with no inserts. It can be noted that tube with inserts gives higher outlet fluid temperature with respect to the plain tube. This is due to the turbulence effect and volumetric heat transfer phenomenon happening with the presence of insert in the tube. Furthermore, additional resistance to fluid flow offered by the insert inside the receiver tube, which results in the fluid being retained for a longer period within the tube. This extended residence time allows for superior heat absorption, causing to a higher temperature rise in the fluid relative to the plain tube, where the fluid flows more quickly.

The figure also illustrates that the outlet temperature of the fluid decreases with rise in the mass discharge rate and the same trend is found for both cases i.e. plain and CRWM tubes. This may be due to the reason that at lesser mass discharge rates, the fluid remains in contact with the

Table 4. Percentage gain in the average Nusselt number at all mass discharge rates

Mass discharge rate (kg/s)	Average Nu Plain tube	Average Nu CRWM tube	% Rise in Nu
0.04	39.41	43.59	10.6%
0.06	41.59	48.93	17.64%
0.08	46.22	55.68	20.46%

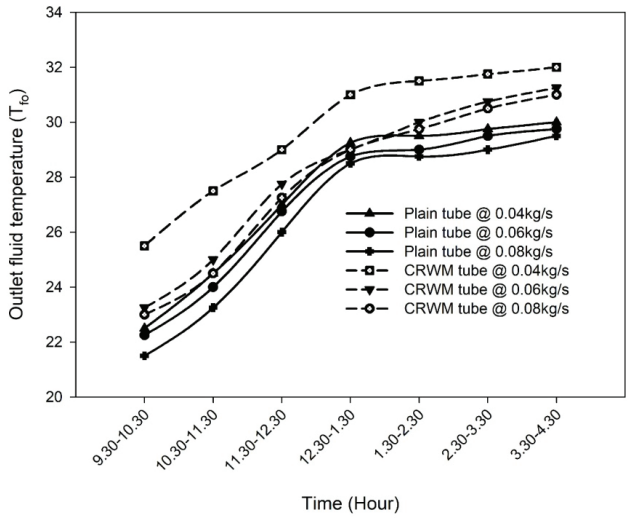

Figure 11. Variation of outlet fluid temperature with time at different discharge rates for plain and CRWM inserted tubes.

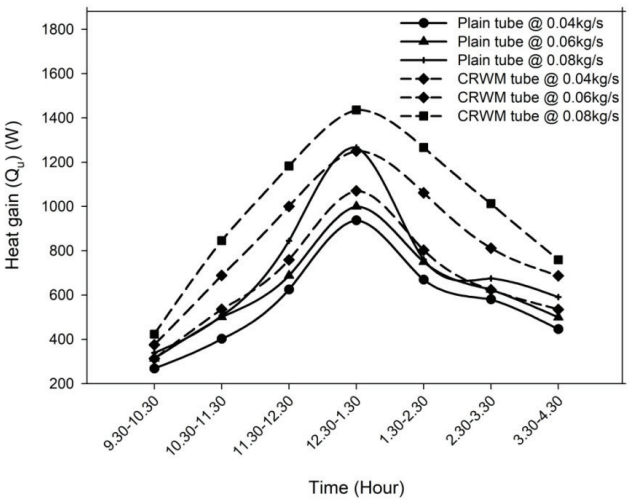

Figure 12. Comparison of heat gain with time at different mass discharge rates for plain and CRWM inserted tubes.

heated surface for a longer duration, allowing more time for heat transfer and leading in a higher outlet temperature. In contrast, at higher mass discharge rates, the fluid moves through the tube more rapidly, reducing the time available for heat absorption, which leads to a lower outlet temperature. However, despite a decrease in solar heat flux after the peak period, the increase in outlet temperature is not as pronounced.

Table 5 presents the percentage increase in the average outlet fluid temperature for both plain and CRWM tubes across different mass discharge rates. The percentage rise in the outlet fluid temperature is 8.1%, 4.42%, and 3.41% at respective mass discharge rates of 0.04, 0.06, and 0.08 kg/s. The output of the experiment signifies that using inserts at lesser mass discharge rates tends to elevated outlet fluid temperature. Varun et al. [37] investigated a similar type of study in PTC having 1500 mm absorber tube length using water as the HTF at mass flow rates of 0.5 to 4 liter per minute. It compared the thermal performance of finned and plain tubes based on outlet fluid temperature, temperature difference, heat transfer, and efficiency. Results showed that the finned tube increased the outlet temperature by 1.23% to 4.75%, with a greater rise at lower flow rates. A similar trend is observed in the present study which supports the effectiveness of inserts in the PTC.

Impact of Mass Discharge Rates on Heat Gain in the Case of Plain and CRWM Inserted Tubes

Figure 12 presents a comparison of heat gain between the plain and CRWM tubes at three different mass discharge rates. The data shows that as the mass discharge rate increases, the useful heat gain also increases, resulting in enhanced thermal efficiency of the PTC. It is observed that the maximum heat gain occurs around solar noon, between 12:30 to 1:30 pm, for both tube configurations, after which the heat gain decreases due to the reduction in solar flux intensity. Additionally, the figure demonstrates that the CRWM tube consistently achieves higher heat gain than the plain tube. This improvement is attributed to the CRWM structure, which better retains the fluid within the tube, allowing for increased fluid retention time and, consequently, more significant heat gain compared to the plain tube.

Table 6 presents the percentage increase in the average heat gain for both plain and CRWM tubes across all mass discharge rates. The heat gain in the tube with inserts shows an 18.1%, 34.2%, and 38.9% increase compared to the plain tube at mass discharge rates of 0.04 kg/s, 0.06 kg/s, and 0.08 kg/s, respectively. These results indicate that higher mass

Table 5. Percentage rise in outlet fluid temperature at different mass discharge rates

Mass discharge rate (kg/s)	Average T_{fo} Plain tube (°C)	Average T_{fo} CRWM tube (°C)	% Rise in T_{fo}
0.04	27.50	29.75	8.1%
0.06	27.14	28.34	4.42%
0.08	26.64	27.55	3.41%

Table 6. Percentage rise in heat gain at different mass discharge rates

Mass discharge rate (kg/s)	Average Q_u Plain tube (W)	Average Q_u CRWM tube(W)	% Rise in Q_u
0.04	561	663	18.1%
0.06	625	839	34.2%
0.08	712	989	38.9%

discharge rates, combined with the use of inserts, lead to improved heat gain compared to the plain tube.

Impact of Mass Discharge Rates on Thermal Efficiency in the Case of Plain and CRWM Inserted Tubes

Figure 13 illustrates a comparison of thermal efficiency between plain and CRWM tube at all three mass discharge rates. The figure indicates that as the mass discharge rate increases, the useful thermal gain also increases, which, in turn, enhances the thermal efficiency of the PTC. It can be noted that the thermal efficiency is maximum at solar noon between 12.30 to 1.30 pm for both tube configurations and then decreases due to a reduction in solar flux intensity, which leads to a drop in the thermal gain and efficiency. The figure also demonstrates that the CRWM tube consistently outperforms the plain tube in terms of thermal efficiency. This improvement can be recognized by the improved heat transfer characteristics of the CRWM tube, which is likely a result of increased turbulence and better fluid mixing due to its corrugated surface design. The corrugations promote more effective interaction between the fluid and the tube surface, causing a reduction in the thermal boundary layer and increasing convective heat transfer.

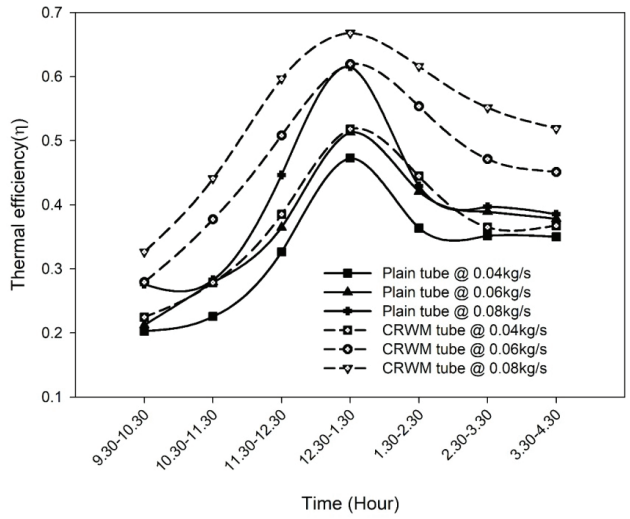

Figure 13. Comparison of thermal efficiency with time at different mass discharge rates for plain and CRWM inserted tubes.

Table 7 presents the percentage increase in the average thermal efficiency for both plain and CRWM tubes across all mass discharge rates. The percentage rise in thermal efficiency is 31.2%, 27.4%, and 12.6% of the tube with insert compared to the plain tube at respective mass discharge rates of 0.08, 0.06, and 0.04 kg/s. This result indicates that a high mass discharge rate and tube with an insert have better thermal efficiency than the plain tube.

Cost Analysis of Evacuated Tube And PTC

For this study, the receiver tube material was chosen as a copper, with an inner and outer diameter of 22 mm and 25 mm with a length of 1300 mm is selected. A borosilicate glass tube, measuring 1000 mm in length, was used to envelop the copper tube with an inner and outer diameter of 47 mm and 50 mm. A vacuum pump was then employed to create a vacuum inside the tube, which was subsequently sealed with a heat-resistant sealing material. The estimated cost of the evacuated receiver tube is found to be Rs. 5300. Table 8 demonstrates the estimated cost of the evacuated tube.

Table 8. Estimated cost of evacuated tube

Material	Cost (Rs)
Copper tube	1800
Glass Cover	500
Sealing material	1500
Vacuum Process	1500
Total Cost	5300

Table 7. Percentage rise in thermal efficiency at different mass discharge rates

Mass discharge rate (kg/s)	Average eff. Plain tube	Average eff. CRWM tube	% Rise in eff.
0.04	0.328	0.369	12.6%
0.06	0.365	0.466	27.4%
0.08	0.405	0.531	31.2%

Table 9. Estimated cost of PTC

Item	Material	Cost (Rs.)
Framework and support	Galvanized iron	17000
Reflector	Mirror	3000
Evacuated tube	Copper and Glass tube	5300
Pyranometer	Class C	46500
Manometer	Inverted acrylic	1500
Thermocouple	K type	5000
Data logger	Modules and PCB	5000
Wire mesh insert	Stainless steel	1000
Miscellaneous	Valves, insulation, fittings	20000
Total Estimated Cost		104300

According to the literature by Chafie et al. [38] the total cost of an evacuated tube mentioned for 4 m length is shown as $ 2127, which is approx Rs. 1,40,000 (considering 1$ = Rs. 66). If the cost of one meter is calculated then it comes to approx. Rs. 35,000. Assuming 15% additional import duties and extra charges on the cost of the evacuated tube will make the tube cost approx. Rs. 40,000 per meter. This comparison shows enormous potential for further examination of the evacuated receiver tube for the small-size PTC, which can be implemented for industrial applications.

In this research, the experimental setup of the PTC was fabricated in the workshop using materials sourced from the local market. Table 9 provides a list of the parts used, along with the associated costs.

CONCLUSION

This paper focuses on optimizing the cost and performance of the evacuated tube used in parabolic solar trough collector. In-house development of the tube with locally available materials in the market approach was used to fabricate the low-cost evacuated receiver tube. A novel notch-based porous insert was fabricated and experimentally examined to improve the thermal retention of the fluid inside the tube. An experimental setup with an aperture area of 2.36 m^2 with a focal length of 0.50 m was designed and constructed to examine the in-house developed tube and porous insert. Water is used as the working fluid, and three mass discharge rates (0.04, 0.06 and 0.08 kg/s) were selected for this study. In six days with different mass discharge rates, experimental readings from the time duration of 9.30 am to 4.30 pm were conducted in the month of January (2025). Parameters such as Nusselt number, outlet fluid temperature, heat gain and thermal efficiency were evaluated to compare performance with and without porous inserts in the tube. The key outcomes of this experimental study are as follows:

1. The solar radiation reading for six different days in the month of January (2025) for the 22°18'N latitude and 70°47'E longitude was measured with the help of a pyranometer. The average solar flux of 863 W/m^2 was noted during the peak solar noon between 12.30 to 1.30 pm.
2. Nusselt number was examined at different mass discharge rates between a plain tube and a tube with an insert. The result reveals that the tube with an insert has a higher Nusselt number than the plain tube at all three mass discharge rates. The rise in Nusselt numbers is 10.6%, 17.64%, and 20.46% for mass discharge rates of 0.04, 0.06, and 0.08 kg/s, respectively.
3. In a similar way, the outlet fluid temperature of the water was studied with and without an insert in the tube at three different mass discharge rates. The experimental results indicate that the tube with the insert has a higher outlet temperature rise of 8.1%, 4.42% and 3.41% for mass discharge rates of 0.04, 0.06 and 0.08 kg/s, respectively.
4. Finally, heat gain and thermal efficiency of the collector were determined for both cases at different mass discharge rates. It was noted that tube with inserts show a superior performance and thermal efficiency rise compared to the plain tube. Additionally, both parameters in tube with inserts show excellent results at higher mass discharge rates. This study also signifies that the tube with an insert improves the thermal retention of the fluid, which ultimately enhances heat gain and thermal efficiency.
5. The cost of the in-house developed evacuated receiver tube was evaluated and compared with existing literature, which shows a positive impact. This type of evacuated tube is more suitable for the small size of parabolic trough collectors, which has high potential for low and medium-temperature industrial applications.

The findings of this study demonstrate a significant enhancement in the efficiency of the collector. This improved efficiency makes the collector highly suitable for a wide range of industrial applications. Its enhanced

performance ensures reliable and cost-effective thermal energy solutions for diverse sectors.

In the future scope, the developed evacuated receiver tube can be further examined for higher temperatures using oil as the working fluid along with the notched circular ring wire mesh insert.

NOMENCLATURE

A_p	Aperture area (m^2)
A_r	Receiver area (m^2)
C_p	Fluid Specific heat (KJ/kg.K)
d_i	Tube internal diameter (m)
d_{go}	Glass outer diameter (m)
F	Focal length (m)
h	Heat transfer coefficient ($W/m^2.K$)
k	Thermal conductivity (W/m.K)
$\dot{m}$	Mass discharge rate (Kg/s)
Pr	Prandtl number
Q_u	Useful heat gain (W)
Re	Reynolds numbers
T_m	Bulk fluid temperature (K)
T_{fi} & T_{fo}	Inlet and outlet fluid temperature (K)
T_{sur}	Receiver surface temperature (K)

Abbreviations

CR	Concentration Ratio
CRWM	Circular ring wire mesh
HTF	Heat transfer fluid
LPM	Liter per minute
PEC	Performance evaluation criteria
PPI	Pores per inch
PTC	Parabolic trough collector
WMTT	Wire mesh twisted tape

Greek symbols

μ	Fluid dynamic viscosity (kg/m.s)
ρ	Fluid density (kg/m^3)
v	Velocity of fluid (m/s)
Φ	Rim angle (°)

ACKNOWLEDGMENT

The authors sincerely thank Marwadi University, Rajkot, for the financial support (Grant No. MU/R&D/21-22/MRP/FT05) to conduct this research project under the Minor Research Project scheme.

AUTHORSHIP CONTRIBUTIONS

Authors equally contributed to this work.

DATA AVAILABILITY STATEMENT

The authors confirm that the data that supports the findings of this study are available within the article. Raw data that support the finding of this study are available from the corresponding author, upon reasonable request.

CONFLICT OF INTEREST

The author declared no potential conflicts of interest with respect to the research, authorship, and/or publication of this article.

ETHICS

There are no ethical issues with the publication of this manuscript.

STATEMENT ON THE USE OF ARTIFICIAL INTELLIGENCE

Artificial intelligence was not used in the preparation of the article.

REFERENCES

[1] Smith J, Brown R. Energy efficiency and urbanization. J Sustain Energy 2022;12(3):45–58.

[2] Lippke F. Parabolic trough technology for solar power plants. Energy Environ Sci 2012;5(2):89–94.

[3] Motwani K, Chotai N, Patel J, Hadiya R. Design and experimental investigation on cut tube absorber for solar parabolic trough collector. Energy Sources Part A 2024;46(1):9173–9192. [CrossRef]

[4] Kennedy CE. Review of Mid- to High-Temperature Solar Selective Absorber Materials. Golden, CO; 2002. [CrossRef]

[5] Motwani K, Patel J. Cost analysis of solar parabolic trough collector for cooking in Indian hostel – a case study. Int J Ambient Energy 2022;43(1):561–567. [CrossRef]

[6] Kasaeian A, Daviran S. Optical and thermal investigation of selective coatings for solar absorber tube. Int J Renew Energy Res 2016;6(1).

[7] Cheng J, et al. Improvement of thermal stability in the solar selective absorbing Mo–Al2O3 coating. Sol Energy Mater Sol Cells 2013;109:204–208. [CrossRef]

[8] Liu J, Lei D, Li Q. Vacuum lifetime and residual gas analysis of parabolic trough receiver. Renew Energy 2016;86:949–954. [CrossRef]

[9] Mahmoud MS, Abbas AS. Solar parabolic trough collector tube heat transfer analysis with internal conical pin fins. J Green Eng 2020;10(10).

[10] Waghole DR, Warkhedkar RM, Kulkarni VS, Shrivastva RK. Experimental investigations on heat transfer and friction factor of silver nanofliud in absorber/receiver of parabolic trough collector with twisted tape inserts. Energy Procedia 2014;45:558–567. [CrossRef]

[11] Raval P. Heat transfer enhancement techniques using different inserts in absorber tube of parabolic trough solar collector: A review. J Therm Eng 2024:1068–1091. [CrossRef]

[12] Hussein AM, Awad AT, Ali HHM. Evaluation of the thermal efficiency of nanofluid flows in flat plate solar collector. J Therm Eng 2024;10(2):299–307. [CrossRef]

[13] Ajbar W, Hernández JA, Parrales A, Torres L. Thermal efficiency improvement of parabolic trough solar collector using different kinds of hybrid nanofluids. Case Stud Therm Eng 2023;42:102759. [CrossRef]
[14] Jaiswal P, et al. Nanofluids guided energy-efficient solar water heaters: Recent advancements and challenges ahead. Mater Today Commun 2023;37:107059. [CrossRef]
[15] Anbarsooz M, Amiri M, Rashidi I, Javadi M. Heat transfer augmentation in solar collectors using nanofluids: A review. Curr Biochem Eng 2020;6(2):72–81. [CrossRef]
[16] Shank K, Tiari S. A review on active heat transfer enhancement techniques within latent heat thermal energy storage systems. Energies 2023;16(10):4165. [CrossRef]
[17] Muter DM, Al-Hadithi MB. Numerical investigation of heat transfer enhancement in parabolic trough solar collector with twisted tape insert. Glob Sci J 2020.
[18] Rawani A. Enhancement in thermal performance of parabolic trough collector with serrated twisted tape inserts. Int J Thermodyn 2017;20(2):111–111. [CrossRef]
[19] Keklikcioglu O, Ozceyhan V. Experimental investigation on heat transfer enhancement in a circular tube with equilateral triangle cross sectioned coiled-wire inserts. Appl Therm Eng 2018;131:686–695. [CrossRef]
[20] Al-Aloosi W, Alaiwi Y, Hamzah H. Thermal performance analysis in a parabolic trough solar collector with a novel design of inserted fins. Case Stud Therm Eng 2023;49:103378. [CrossRef]
[21] Zaboli M, Ajarostaghi SSM, Saedodin S, Pour MS. Thermal performance enhancement using absorber tube with inner helical axial fins in a parabolic trough solar collector. Appl Sci 2021;11(16):7423. [CrossRef]
[22] Waramit P, Chanmak P, Peamsuwan R, Krittacom B. Forced convection enhancement of air flowing inside circular pipe with varying the pitch (P) of wire-mesh porous media. Energy Rep 2021;7:70–82. [CrossRef]
[23] Raval P, Ramani B, Chotai NJ, Motwani K. Wire mesh-based heat transfer enhancement in absorber tube of solar collector-An experimental study. Int J Thermofluids 2024;24:100878. [CrossRef]
[24] Thapa S, Samir S, Kumar K. Performance evaluation of solar parabolic trough receiver using multiple twisted tapes with circular perforation and delta winglet. Proc Inst Mech Eng Part E J Process Mech Eng 2022;236(4):1296–1307. [CrossRef]
[25] Ioannides MG, Cammi A, Savoldi L. Improving the overall thermal performance of parabolic trough solar collectors using porous media. Renew Energy Power Qual J 2024;19(5). [CrossRef]
[26] Afsharpanah F, Sheshpoli AZ, Pakzad K, Ajarostaghi SSM. Numerical investigation of non-uniform heat transfer enhancement in parabolic trough solar collectors using dual modified twisted-tape inserts. J Therm Eng 2020:133–147. [CrossRef]
[27] Jain PK, Chaurasiya PK, Verma TN, Tiwari D. Investigation of the heat discharge from a solar-powered air heater with distinctive dual arc artificial roughness. Sustain Energy Technol Assess 2023;60:103543. [CrossRef]
[28] Natarajan K, Thokchom SS, Verma TN, Nashine P. Convective solar drying of Vitis vinifera & Momordica charantia using thermal storage materials. Renew Energy 2017;113:1193–1200. [CrossRef]
[29] Chaurasiya PK, et al. A review of techniques for increasing the productivity of passive solar stills. Sustain Energy Technol Assess 2022;52:102033. [CrossRef]
[30] Khashaei A, Ameri M, Azizifar S. Heat transfer enhancement and pressure drop performance of Al2O3 nanofluid in a laminar flow tube with deep dimples under constant heat flux: An experimental approach. Int J Thermofluids 2024;24:100827. [CrossRef]
[31] Morka JC, Molua OC, Egheneji A, Edobor M, Ighrakpata FC. Experimental study corrosion parameters of copper as an eco-friendly heat collector for solar water heaters. J Geogr Environ Earth Sci Int 2023;27(5):49–55. [CrossRef]
[32] Gao XH, Guo ZM, Geng QF, Ma PJ, Liu G. Structure, optical properties and thermal stability of TiC-based tandem spectrally selective solar absorber coating. Sol Energy Mater Sol Cells 2016;157:543–549. [CrossRef]
[33] Selvakumar N, Rajaguru K, Gouda GM, Barshilia HC. AlMoN based spectrally selective coating with improved thermal stability for high temperature solar thermal applications. Sol Energy 2015;119:114–121. [CrossRef]
[34] Kalogirou SA. Solar thermal collectors and applications. Prog Energy Combust Sci 2004;30(3):231–295. [CrossRef]
[35] Cengel YA, Ghajar AJ. Heat and Mass Transfer. McGraw-Hill; 2014.
[36] Limboonruang T, Oyinlola M, Harmanto D, Bunyawanichakul P, Phunapai N. Optimizing solar parabolic trough receivers with external fins: An experimental study on enhancing heat transfer and thermal efficiency. Energies 2023;16(18):6520. [CrossRef]
[37] Varun K, Arunachala UC, Elton DN. Trade-off between wire matrix and twisted tape: SOLTRACE® based indoor study of parabolic trough collector. Renew Energy 2020;156:478–492. [CrossRef]
[38] Chafie M, Aissa MFB, Bouadila S, Balghouthi M, Farhat A, Guizani A. Experimental investigation of parabolic trough collector system under Tunisian climate: Design, manufacturing and performance assessment. Appl Therm Eng 2016;101:273–283. [CrossRef]